

8th U. S. National Combustion Meeting
Organized by the Western States Section of the Combustion Institute
and hosted by the University of Utah
May 19-22, 2013

Laminar Flame Speed, Markstein Length and Flame Chemistry of the Butanol Isomers from 1 atm to 5 atm

Fujia Wu and Chung K. Law

*Department of Mechanical and Aerospace Engineering
Princeton University, Princeton, New Jersey 08544*

Laminar flame speeds and Markstein lengths for n-butanol, s-butanol, i-butanol and t-butanol at pressures from 1 atm to 5 atm were experimentally measured in a heated, dual-chamber vessel. Results at all pressures show that n-butanol has the highest flame speeds, followed by s-butanol and i-butanol, and then t-butanol, which quantitatively agree reasonably well with the computed results using the recent mechanism of Sarathy and co-authors. Results further show that while the isomers have different Markstein lengths, they have similar Markstein numbers which is the appropriate nondimensional parameter to quantify flame stretch. Investigations on thermal effects, reaction rate sensitivities, intermediate species distributions and reaction paths subsequently demonstrate that kinetic effect is the primary reason for the ordering of the flame speed. Specifically, since s-butanol, i-butanol and t-butanol all have branched molecular structures, they crack into relatively stable branched intermediate species, such as iso-butene, iso-propenol and acetone, with the resulting flame speeds depending on the extent of fuel molecule branching.

1. Introduction

Butanol holds much potential as a significant alternative transportation fuel. Compared to methanol and ethanol, butanol not only has a diverse source of feedstock, but it also has more desirable fuel properties such as higher energy density, miscibility with gasoline and diesel, and less corrosion. In order to evaluate and implement butanol as a practical transportation fuel, it is therefore important to understand its combustion characteristics.

There are four butanol isomers, namely normal butanol (*n*-butanol or 1-butanol), secondary butanol (*s*-butanol or 2-butanol), iso-butanol (*i*-butanol) and tertiary butanol (*t*-butanol). Most previous studies have focused on *n*-butanol, with *s*-butanol, *i*-butanol and *t*-butanol receiving considerably less attention. It is noted [1] that *s*-butanol and *i*-butanol are also produced in biological fermentation processes, and that *t*-butanol is a petrochemical product which has been used for decades as an octane enhancer in gasoline. Therefore studying the combustion characteristics of the four butanol isomers are all useful and important.

The laminar flame speed of a combustible mixture is an important global combustion parameter which also contains the chemical information of the mixture such that it can be used to partially

validate chemical kinetics models developed for the mixture. For the butanol isomers, not many data other than those of *n*-butanol have been reported, and most of the measurements were conducted only at atmospheric pressure. Specifically, laminar flame speeds were reported by Sarathy *et al.*[2] for *n*-butanol at 0.89 atm pressure and initial temperature of 350 K; by Veloo *et al.*[3] for the four isomers at 1 atm and 343 K; by Liu *et al.*[4] for *n*-butanol and *i*-butanol at 1 atm and 2 atm and initial temperature of 353 K; and by Gu *et al.* [5-8] for *n*-butanol from 1 atm to 2.5 atm, *t*-butanol from 1 atm to 5 atm, and stoichiometric mixtures of the four isomers with air up to 7.5 atm.

The present investigation aims to first acquire additional data on the laminar flame speed and the associated Markstein length for all the butanol isomers at atmospheric and elevated pressures. By using expanding spherical flames, we have subsequently measured the laminar flame speeds of *n*-butanol, *s*-butanol, *i*-butanol and *t*-butanol at 1 atm, 2 atm and 5 atm at elevated initial temperatures. These data can be used to validate and develop the kinetic mechanisms for the butanol isomers. In particular, since the present investigation yields validation data sets for all the isomers across a wide range of identical experimental conditions, we have conducted a consistent comparison of the reactivity among them, yielding useful insight into the controlling kinetics.

2. Methods

Since detailed specification of the experimental apparatus, procedure and data analysis were reported in previous publications [9,10], only a brief description is provided here. The apparatus consists of a cylindrical chamber radially situated within another cylindrical chamber of substantially larger volume. The wall of the inner chamber is fitted with a series of holes that can be mechanically opened and closed to allow the union and separation of the gases. The desired equivalence ratio in the inner chamber is obtained by monitoring the partial pressures of the gases in the inner chamber. The outer chamber is filled with a mixture of inert gases to match the pressure and density of the gas in the inner chamber. Spark ignition and opening the holes between the inner and outer chambers occur concurrently, resulting in an expanding spherical flame that propagates throughout the inner chamber in essentially an isobaric environment. The outer chamber is covered with silicon electrical heaters, hence enabling it to act as an oven to uniformly heat the inner chamber to a given temperature. The flame surface is visualized using a pin-hole Schlieren system coupled to a high-speed camera.

Tracking the flamefront yields the history of the radius of the spherical flame as a function of time. For extrapolation of the laminar flame speed, we employ the nonlinear relation recently derived by Kelley *et al.*[11],

$$S_b^0 t + C = r_f + 2L_b \ln r_f - \frac{4L_b^2}{r_f} - \frac{8L_b^3}{3r_f^2} \quad (1)$$

where S_b^0 is the adiabatic, unstretched gas speed of the burned mixture relative to the flame, r_f the flame radius, L_b the Markstein length at the burned mixture side and t the time. Equation 1 contains up to the third-order accuracy in terms of the inverse flame radius. For flame speed measurements using expanding spherical flames, the data selected for extrapolation need to be within a certain radius range in that the small and large radius data are respectively affected by the influence of ignition and the chamber confinement, as discussed in details in Refs. [12-15]. For our experimental setup and the fuels studied, a conservative assessment of this range is between radii of 1.0 to 1.8 cm. Based on repeated measurements and the sensitivity of slight variation of the data selection, reported laminar flame speeds in this paper have an uncertainty of approximately ± 2 cm/sec. Table 1 contains the pertinent information of the fuels considered in the current investigation.

Chemical name	Molecular formula	Structure	Purity
<i>n</i> -butanol (1-butanol)	C ₄ H ₉ OH		99+%
<i>s</i> -butanol (2-butanol)	C ₄ H ₉ OH		99+%
<i>i</i> -butanol (<i>iso</i> -butanol)	C ₄ H ₉ OH		99+%
<i>t</i> -butanol (<i>tert</i> -butanol)	C ₄ H ₉ OH		99+%

Table 1 Fuel specific properties

Laminar flame speeds were calculated using the Chemkin Premix code [16], which simulates one-dimensional, steady, planar flames. All calculation were performed using the high temperature version of the detailed chemical kinetic model recently developed by Sarathy *et al.*[17], and as such will not be separately specified. Since the mechanism includes pressure dependent reactions with rate constant formulated by the PLOG function which is not accepted by Chemkin II or III, we used the modified Chemkin II interpreter and library developed by Gou *et al.*[18], which implements the PLOG formulation for pressure-dependent reactions. The calculation incorporated adaptive gridding, which was refined until a grid-independent solution was found.

The calculation results can be used to test the validity of the kinetic model. As shown in the next section, the mechanism of Sarathy *et al.*[17] yields reasonably good agreement with the experiment

for the conditions considered herein, implying that it can be further used as a tool to analyze and interpret the flame characteristics of butanol isomers.

3. Results and Discussion

3.1 Laminar flame speeds

Figure 1 plots the measured flame speeds at 1, 2 and 5 atm. For all the isomers, measurements at 1 and 2 atm were conducted with initial gas temperature of 353 K and standard synthesized air as oxidizer. Experimentation at higher pressures was however limited by fuel condensation as more fuel vapor is needed at higher pressures. To circumvent this difficulty, we chose the initial gas temperature to be 373 K, and used an oxidizer with reduced oxygen concentration and a mixture of argon and helium as bath gas ($O_2:Ar:He = 13:38.1:48.9\%$ by mole). This renders the fuel vapor pressure as low as possible while the mixture also has a favorable effective Lewis number for accurate extrapolation, noting that using pure argon or helium as bath gas will cause the Lewis number to be either too small or too large. With these provisions, we were able to acquire data up to 5 atm.

Figure 1 plots the measured laminar flame speeds for all four butanol isomers. It is seen that *n*-butanol has the highest flame speeds at all pressures, followed by *s*-butanol and *i*-butanol, with *t*-butanol having the lowest flame speeds. The flame speed difference between *s*-butanol and *i*-butanol is only 1% for all conditions, which is less than the experiment uncertainty. The flame speed difference between *n*-butanol and *i*-butanol (or *s*-butanol) is 6% at 1 atm and 10% at 5 atm, while the difference between *n*-butanol and *t*-butanol is 20% at 1 atm and 26% at 5 atm.

Figure 1 also plots the computed flame speeds for all four isomers. Overall satisfactory agreement is seen for all pressures. The model has the closest agreement for *t*-butanol and *i*-butanol, with less than 2% difference with the experiments. For *n*-butanol and *s*-butanol, the model shows slightly higher values, about 2-3% and 3-6% respectively. The model also shows that the flame speed of *s*-butanol is 5% to 9% higher than that of *i*-butanol, while the experiments yield almost the same flame speeds for *s*-butanol and *i*-butanol.

Figure 2 plots the comparison between the current measurements with those by Veloo *et al.*[3] at 1 atm with air as the oxidizer for all butanol isomers. The measurements by Veloo *et al.*[3] were conducted using the counterflow flames, for the experimental conditions are the same to the present one except the unburned gas temperature is lower by 10 K. As indicated in the caption of Figure 2, a correction was performed to account for this 10 K difference before the comparison. It is seen that the measurements of Veloo *et al.*[3] are higher than the present values by 5-8% for *n*-butanol, *s*-butanol and *i*-butanol, whereas the difference in the *t*-butanol data is well within experimental uncertainty (< 2%). In addition, for *n*-butanol, *s*-butanol and *i*-butanol the peak flame speed in Veloo

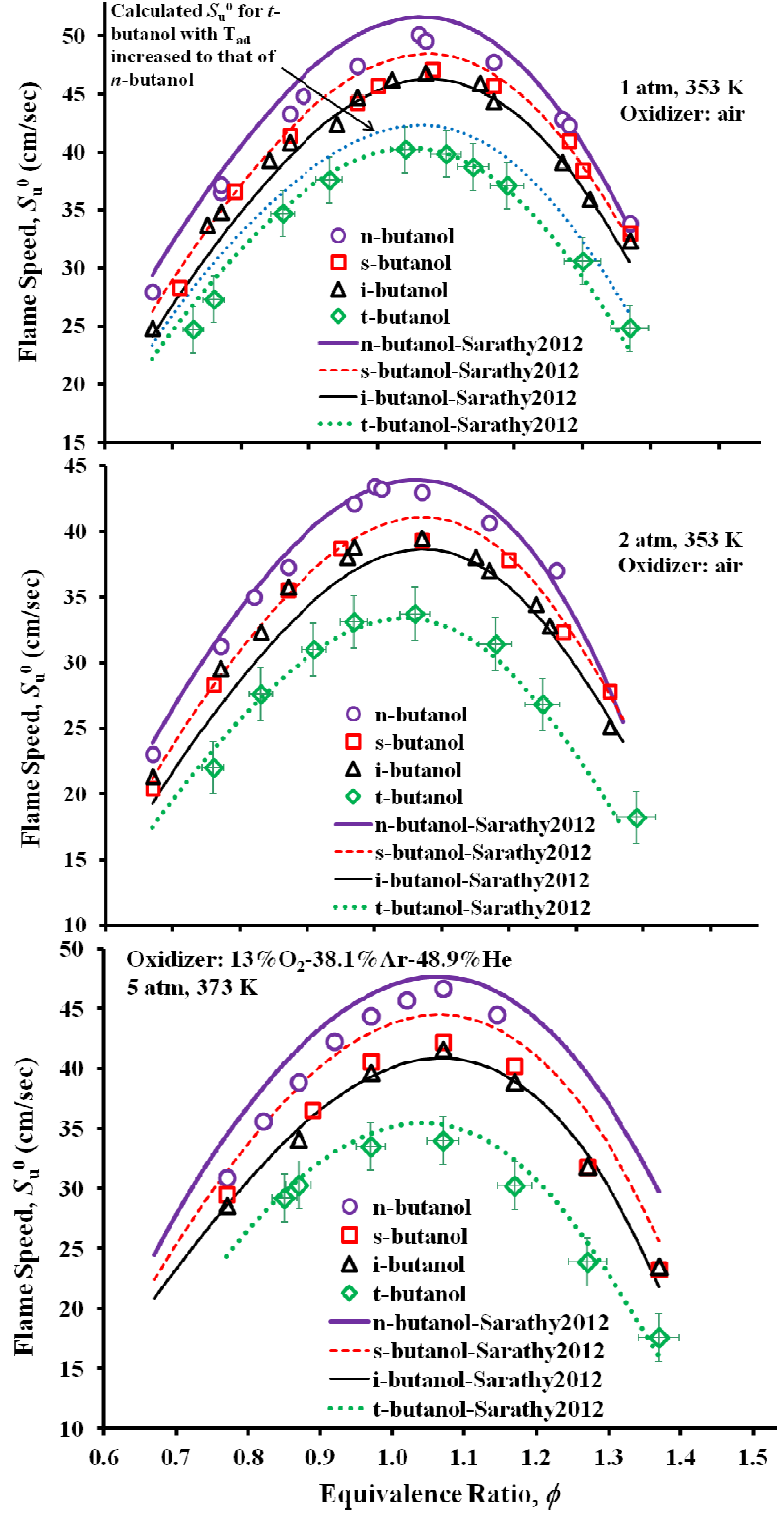


Figure 1. Measured flame speeds, S_u^0 , of butanol isomers at 1 atm, 2 atm, and 5 atm. Error bars are plotted only on the data for *t*-butanol for clarity. Computed flame speeds using the mechanism of Sarathy *et al.*[17] are shown for comparison.

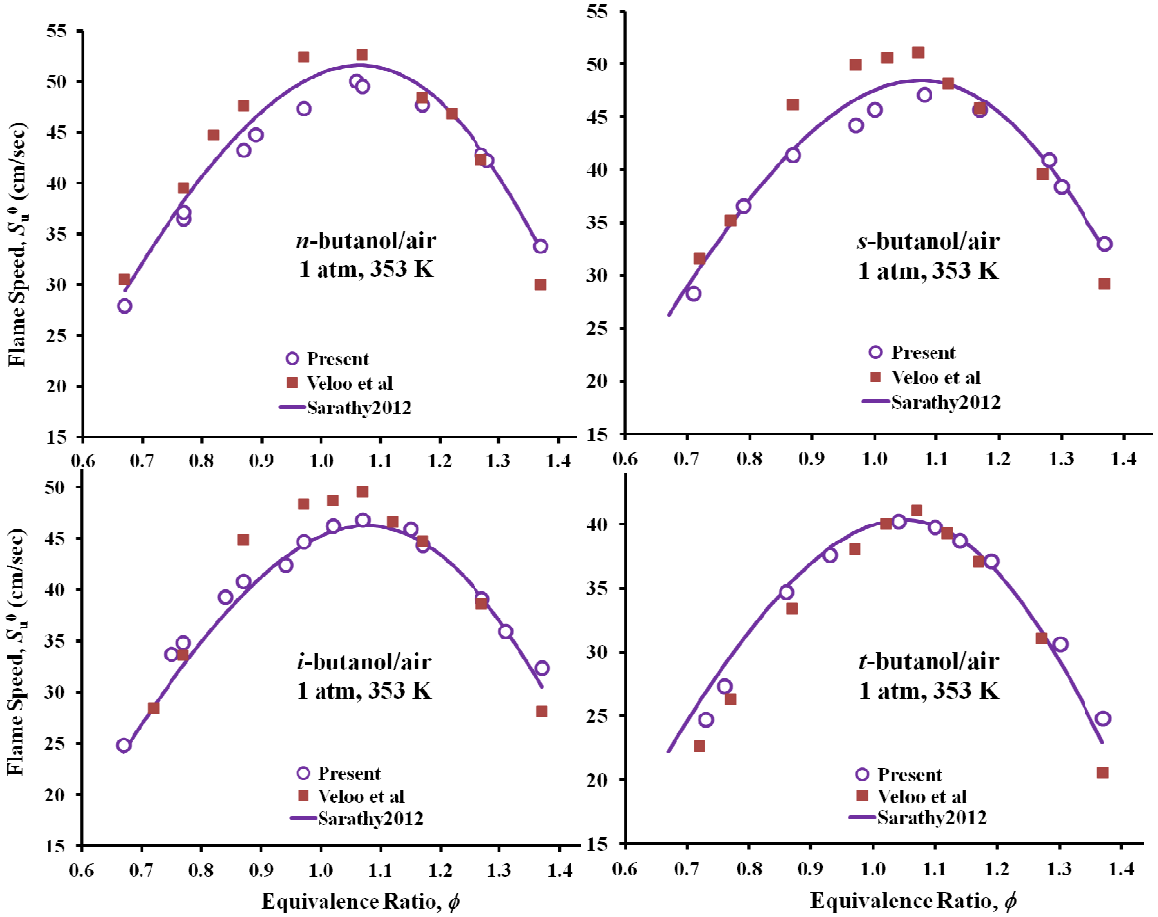


Figure 2. Comparison of present measurements with those by Veloo *et al.*[3] at 1 atm. Measurements by Veloo *et al.*[3] were conducted at initial temperature of 343 K. An empirical relation $s_u^0 \sim T_u^{1.8}$ was applied on the data of Veloo *et al.*[3] to account for the small difference in the initial temperatures from 353 K.

et al.[3] is at $\phi \approx 1.05$, while the calculations and the present measurements peak around $\phi \approx 1.1$.

It is seen that the present experiment, measurements by Veloo *et al.*[3] and calculations show a consistent trend in the flame speed of butanol isomers: *n*-butanol > *s*-butanol > *i*-butanol > *t*-butanol. This trend remains the same as the pressure increases from 1 atm to 5 atm. We note that in Gu *et al.*[6] a different trend is noted as the pressure increases: compared to *n*-butanol, the flame speed of *s*-butanol and *i*-butanol are lower by 13% at 1 atm, but higher by 11% at 5 atm and 7.5 atm. This switch in the flame speed trend as pressure increases is not seen in the present measurements as well as in the calculations.

3.2 Markstein lengths

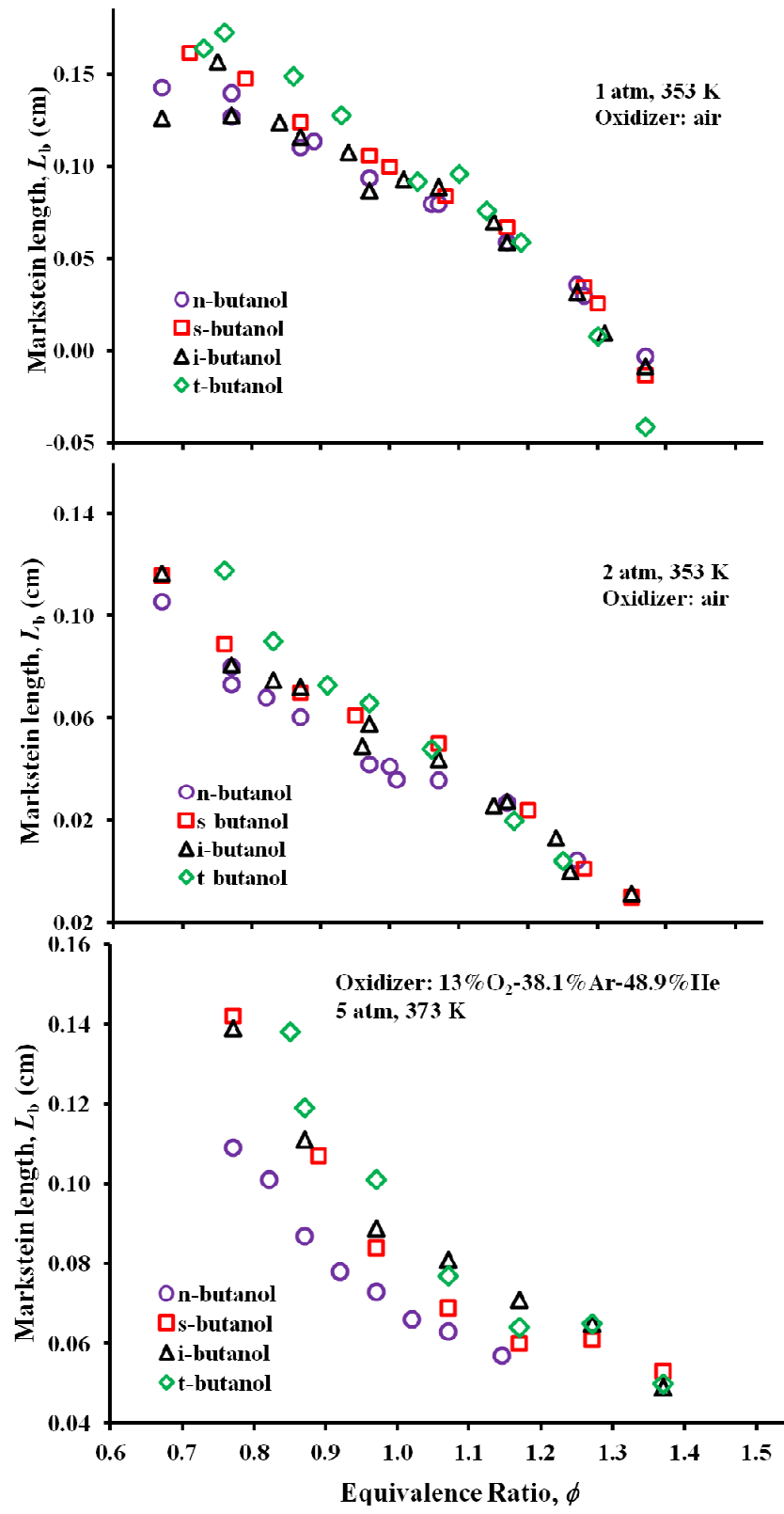


Figure 3. Measured Markstein lengths, L_b , of butanol isomers at 1 atm, 2 atm, and 5 atm.

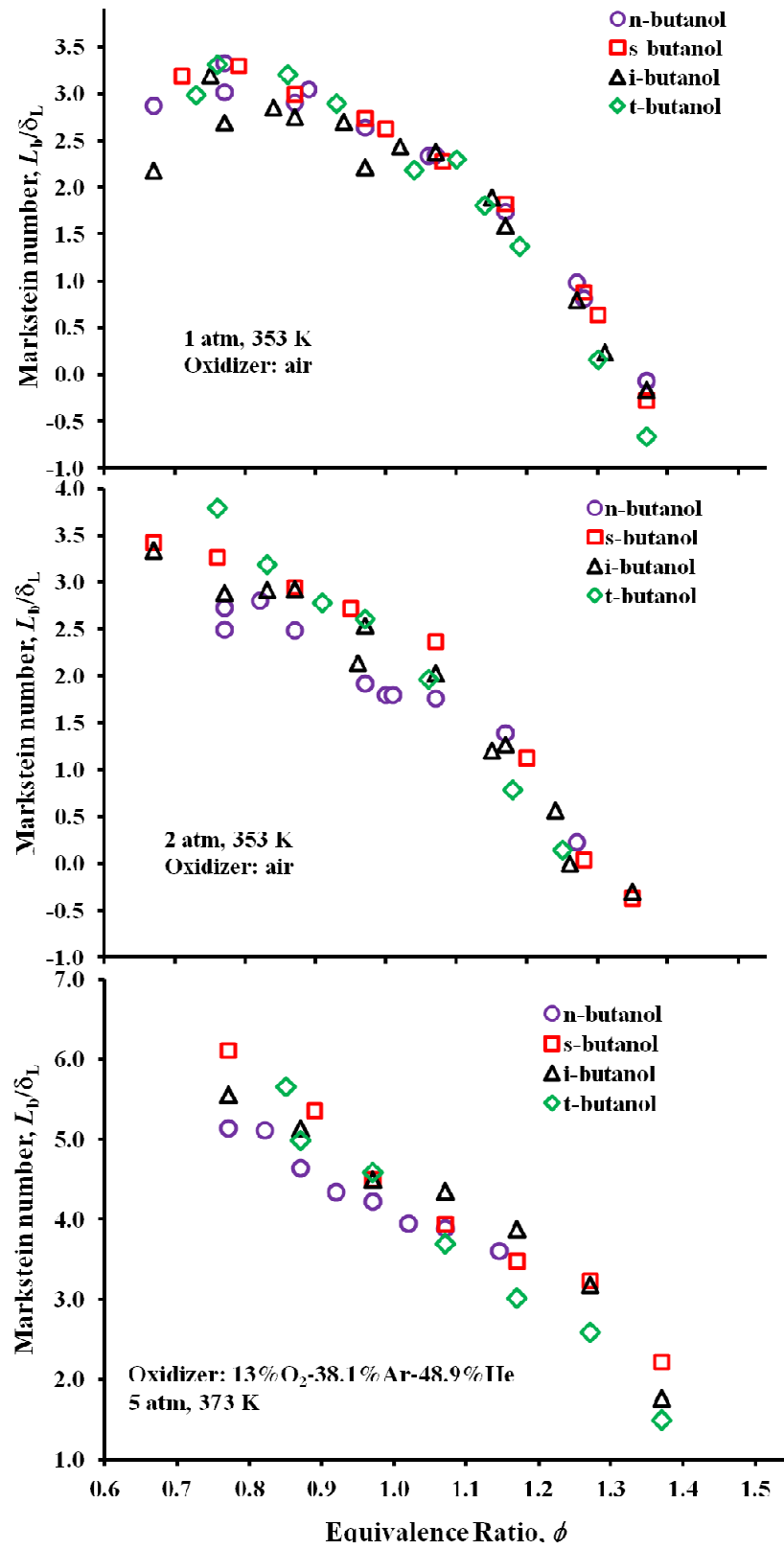


Figure 4. Measured Markstein numbers, L_b/δ_L , of butanol isomers at 1 atm, 2 atm, and 5 atm.

Figure 3 plots the Markstein lengths at the burned mixture side, L_b , corresponding to the laminar flame speed measurements shown in Figure 1. This value directly results from the extrapolation using Equation 1. It is seen that the Markstein lengths of all the butanol isomers have similar values at 1 and 2 atm and with air as the oxidizer, with differences smaller than the experimental uncertainty. However, at 5 atm and with an oxygen-helium-argon mixture as the oxidizer, the Markstein lengths of *n*-butanol are considerably lower than those of the other three isomers.

To reconcile the above difference, we first note that since the Markstein length is a dimensional quantity, it may not be appropriate to extract the underlying physical information through quantitative comparison of its values obtained from different situations. Indeed, the relevant parameter that characterizes the sensitivity of flame speed to stretch is the Markstein number, which is the Markstein length normalized by the flame thickness. Since the 5 atm experiments were conducted using different inerts, and since the flame thickness also decreases with increasing pressure, it behoves us to perform the comparison on the basis of the Markstein number instead of the Markstein length. Figure 4 therefore plots the Markstein numbers for the isomers, with the flame thickness δ_L evaluated using the gradient method. It is then seen that the Markstein numbers of *n*-butanol at 5 atm and with an oxygen-helium-argon mixture as the oxidizer are almost the same as those of the other isomers. This indicates that the smaller Markstein length for *n*-butanol is caused by its smaller flame thickness as compared to the other isomers. In Figure 4 it is also seen that the four isomers also have similar Markstein numbers at 1 atm and 2 atm with air as oxidizer. These results indicate that despite the isomers having distinct flame speeds, the effects of their transport characteristics on the global combustion parameters are similar.

4. Discussions

4.1 Thermal effects

We shall next endeavor to identify the fundamental reasons governing ordering of the laminar flame speeds among the isomers. From flame theory, the laminar flame speed is determined by three aspects of the mixture: thermal effects, transport effects and kinetic effects. Figures 3 and 4 have shown that all four isomers have similar transport effects as they have similar Markstein numbers. We shall therefore investigate the thermal and kinetic effects.

Figure 5 plots the adiabatic flame temperatures of the four isomers at 1 atm and 5 atm. It is seen that all the isomers have very close adiabatic flame temperatures, with that of *n*-butanol being the highest, followed by *s*-butanol, *i*-butanol and then *t*-butanol. However, the differences among them are small. Specifically, the difference between *t*-butanol and *n*-butanol is around 20 K at lean and stoichiometric conditions and around 30 K on the rich side. To quantify the effect of such a thermal difference, additional cases were calculated for *t*-butanol/air at 1 atm with the adiabatic temperature increased to that of *n*-butanol/air by slightly reducing the nitrogen concentration. The calculated

results are plotted on Figure 1. The increase in flame speed by this temperature adjustment is about 2 cm/sec, only 1/5 of the difference between the calculated flame speeds of *n*-butanol and *t*-butanol. This indicates that flame temperature is not the main reason for the flame speed difference among the isomers.

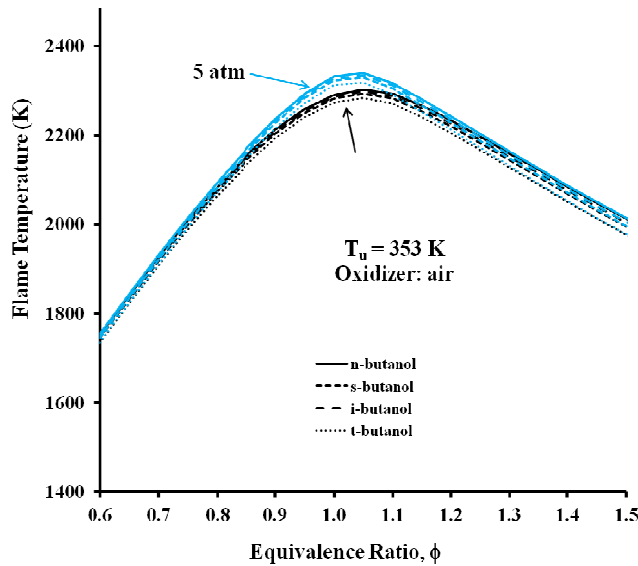


Figure 5.Computed temperature and heat release profiles of 1-D planar flame for the butanol isomers.

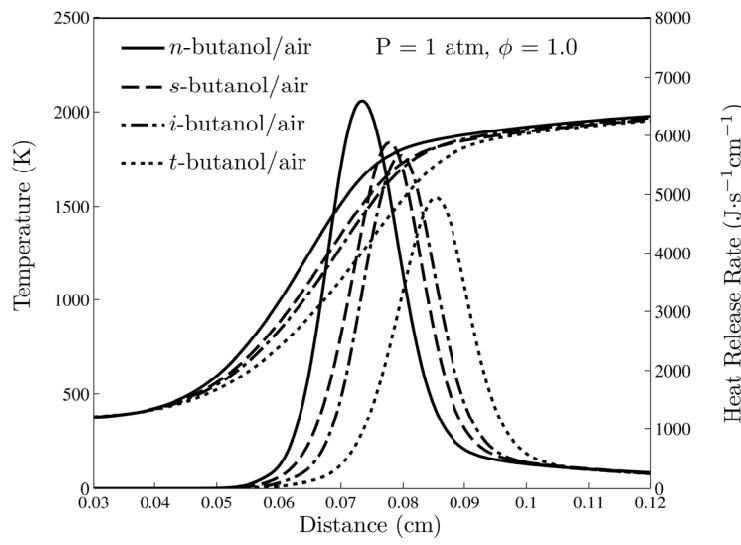


Figure 6.Computed temperature and heat release profiles of 1-D planar flame for the butanol isomers.

Figure 6 plots the temperature and heat release profiles of the one-dimensional planar flames for the isomers at 1 atm with air as the oxidizer. It is seen that the flame temperatures upstream ($x < 0.04$ cm) and downstream ($x > 0.1$ cm) of the flame zone for the four flames are almost identical while they differ significantly within the flame zone ($0.04 \text{ cm} < x < 0.1 \text{ cm}$). This difference in the temperature profiles is associated with the difference in the heat release rates, with the peak heat release rate for *n*-butanol being the highest, followed by *s*-butanol, *i*-butanol and then *t*-butanol; the ordering coincides with that of the laminar flame speeds.

4.2 Sensitivity analysis

To investigate the kinetic effects, we first conduct sensitivity analysis of the rate constants, recognizing that reactions with high sensitivity on the burning rate are rate limiting. Figure 7 plots the 20 reactions that have the largest normalized rate constant sensitivity coefficients for all isomers at 1 atm with air as the oxidizer. It is seen that for all isomers the flame speed is sensitive mostly to the kinetics of hydrogen, carbon monoxide, and the small hydrocarbons. The fuel specific reactions are not the most rate limiting ones, with only one exception, namely the reaction involving *iC₄H₇* and *iC₄H₈*, which shows noticeable sensitivity on the *t*-butanol flame speed. This heightened sensitivity on hydrogen and small hydrocarbon kinetics is similar to many other heavy hydrocarbons [9,10,20], indicating that there is no fundamental difference between the kinetics of butanol isomers including *t*-butanol with that of the other heavy hydrocarbons.

4.3 Intermediate species distributions

Although the rate-limiting reactions are similar, the values of their sensitivity coefficients are different among the isomers. This is due to the different distributions of species concentrations of hydrogen and the small hydrocarbons. To visualize such a difference, Figure 8 plots the peak species concentrations for *s*-butanol, *i*-butanol and *t*-butanol normalized by those of *n*-butanol, for representative species of various size and structure. From Figure 8, it is seen that the species distributions become more distinct as the molecule size increases. The relative differences between concentrations of small radicals, such as H, OH, and CO, CH₄ are within 50%, while the concentration ratios of C₂-C₃ species range from 0.1 to 10. The concentration ratios of species for C₄ species range from 0.001 to 1000.

A few observations can be made from Figure 8. First, the ranking of the concentrations of H, OH and O is consistent with the flame speed: *n*-butanol has the highest concentrations, followed by *s*-butanol and *i*-butanol, and then *t*-butanol. The concentrations of H, O and OH of *t*-butanol are lower than those of *n*-butanol by 22%, 16% and 7%, respectively. Such differences are much smaller compared to those of the larger species, but they have considerable effects on the flame speeds because the reactions involving them are the rate-limiting ones (the largest sensitivity coefficients).

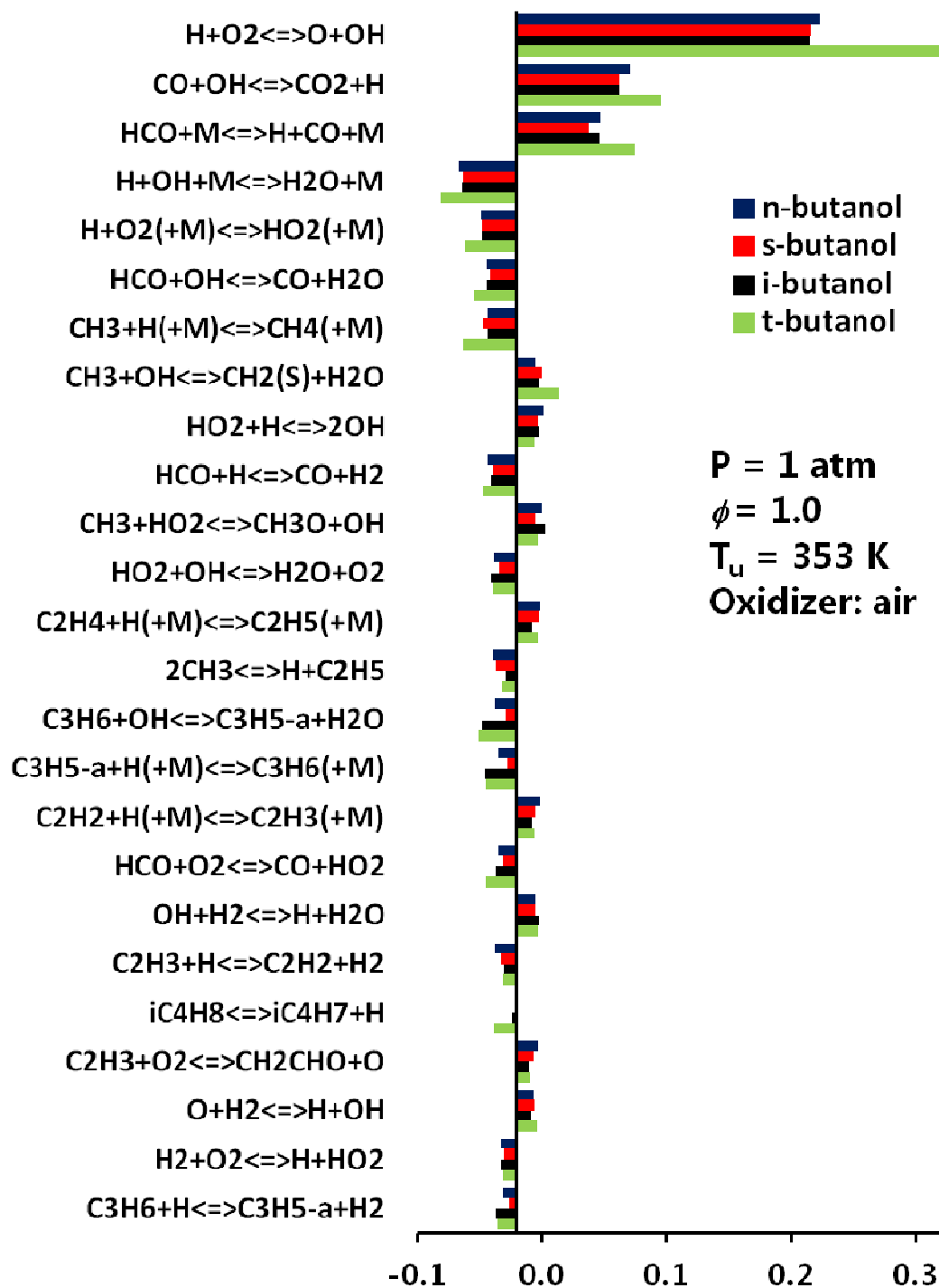


Figure 7. Rate constant sensitivity coefficients on burning rate of the butanol isomers, calculated with the Chemkin Premix code [16].

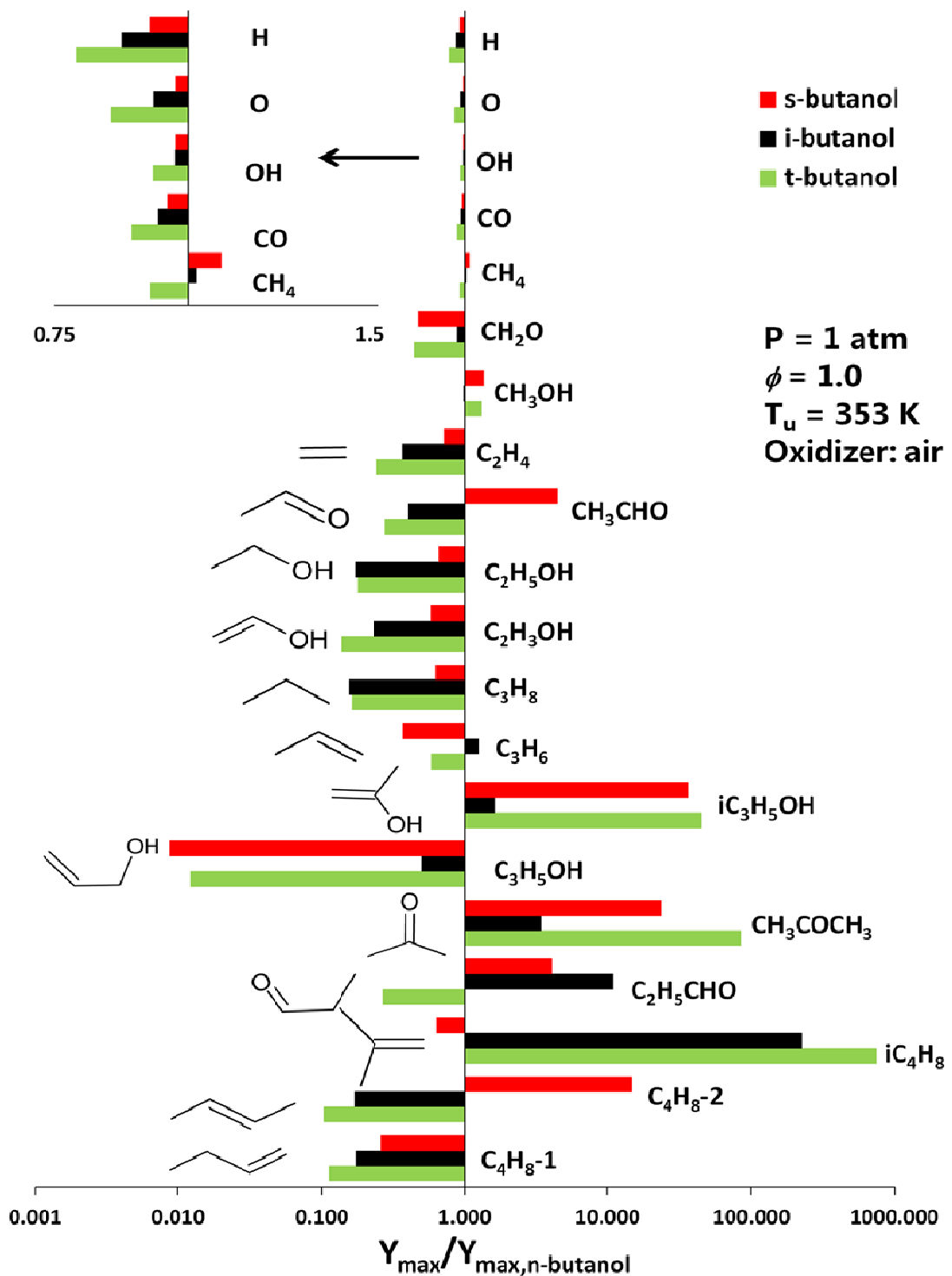


Figure 8. Peak species concentration in 1-D planar flame for *s*-butanol, *i*-butanol and *t*-butanol scaled by the corresponding value for *n*-butanol, calculated with the Chemkin Premix code [16].

Second, *i*-butanol and *t*-butanol have much smaller amount of the C₂-C₃ species such as C₂H₄, C₃H₈, C₂H₅OH, C₂H₅OH and CH₃CHO. Their concentrations are about 10-20% of those of *n*-butanol. Exceptions are the C₃H₆ concentration of *i*-butanol, which is slightly higher than that of *n*-butanol. Concentrations of C₂-C₃ species for *s*-butanol are lower than those of *n*-butanol, but higher than *i*-butanol and *t*-butanol, about 50% of the values of *n*-butanol. The exception is the concentration for *s*-butanol, which is 4.5 times higher than that of *n*-butanol. As will be shown next, the lower C₂-C₃ species concentrations for *s*-butanol, *i*-butanol and *t*-butanol are due to the higher concentrations of intermediate branched C₄ species, which are kinetically slower to be cracked. The C₂ species such as C₂H₄ have high reactivity because its further oxidization bypasses the stable species CH₃ and CH₄. This is also consistent with the lower flame speeds for *s*-butanol, *i*-butanol and *t*-butanol.

As the molecule size increases, more different species distribution is seen among the isomers. For the C₄ hydrocarbons and C₃ oxygenated species, it is seen that, compared to *n*-butanol, *s*-butanol, *i*-butanol and *t*-butanol has significantly more branched species and less straight chain species. Specifically, in *i*-butanol flame there is considerably more *iso*-butene than 1-butene and 2-butene. *iso*-Butene is notably stable and has slow flame speeds as noted in many previous studies [20,21]. In *s*-butanol flames, the concentration of *iso*-butene is almost the same as that in *n*-butanol; however, there are considerably more acetone (CH₃COCH₃) and *iso*-propenol (iC₃H₅OH), in contrast to the corresponding straight chain species, propanal (C₂H₅CHO) and *n*-propenol (C₃H₅OH). As shown in [17,22], acetone and *iso*-propenol can exchange through tautomerization reaction or isomerization reactions with radical, and they both are relatively stable intermediate species. This therefore explains the lower flame speed of *s*-butanol relative to *n*-butanol. In *t*-butanol flame, the concentrations of all branched species (*iso*-butene, acetone and *iso*-propenol) are the highest, and the concentrations of straight chain species (1-butene, 2-butene, propanal and *n*-propenol) are almost the lowest. This explains why *t*-butanol has the lowest flame speeds.

4.4 Reaction path analysis

The distinct distributions of intermediate species among the isomers are clearly due to their different molecular structures. Figures 9-12 plot their initial fuel cracking reaction paths in the one-dimensional planar flame. For each fuel, the main initial fuel cracking path is the H-abstraction reaction, forming various hydroxybutyl radicals which further crack into smaller species depending on which β bond is the weakest. The calculation in [6] shows the following ordering of bond dissociate energies in butanol fuel molecules: O-H bond (104~107 kcal/mol) > terminal C-H bond (100~103 kcal/mol) > inner C-H bond (97~99 kcal/mol) > C-O bond (93~96 kcal/mol) > C-C bond (85~90). The bond energies at the β position in hydroxybutyl radicals will be different but the ordering remains. This indicates that in the cracking process, the C-O bonds are more likely to break compared to the C-H and O-H bonds.

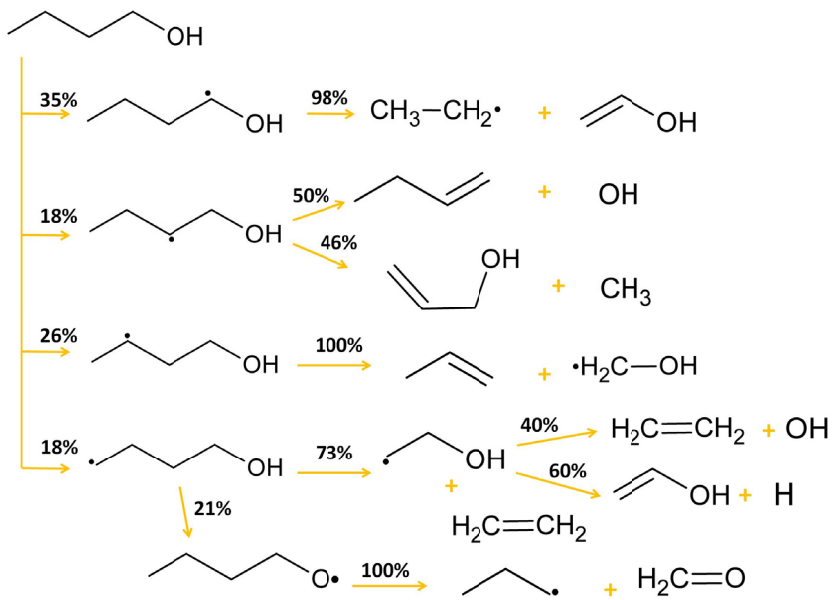


Figure 9. Fuel cracking path of *n*-butanol in the stoichiometric 1-D planar flame with air at 1 atm and initial temperature of 353 K.

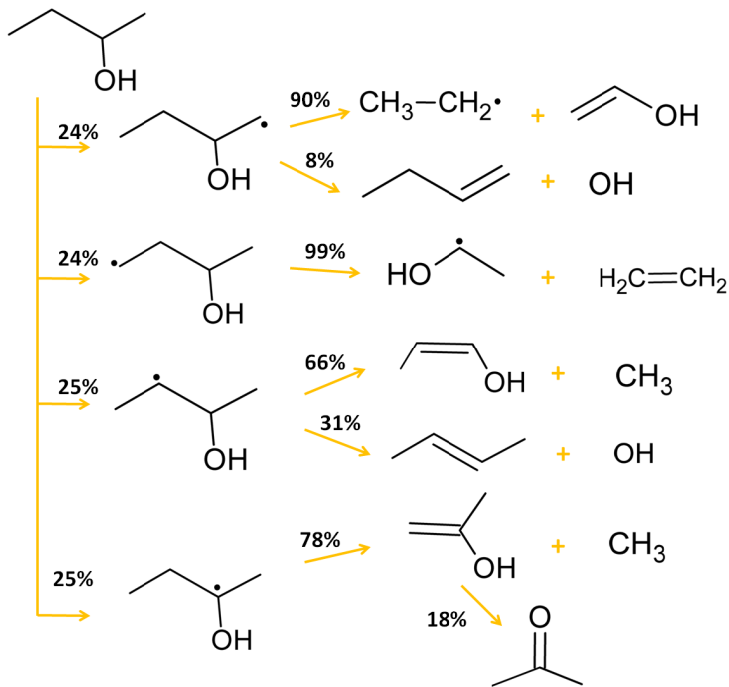


Figure 10. Fuel cracking path of *s*-butanol in the stoichiometric 1-D planar flame with air at 1 atm and initial temperature of 353 K.

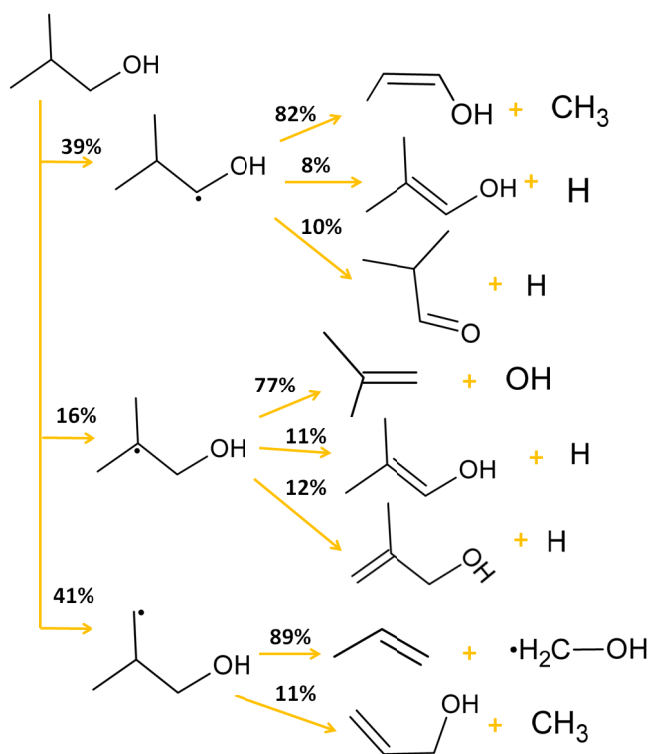


Figure 11. Fuel cracking path of *i*-butanol in the stoichiometric 1-D planar flame by with air at 1 atm and initial temperature of 353 K.

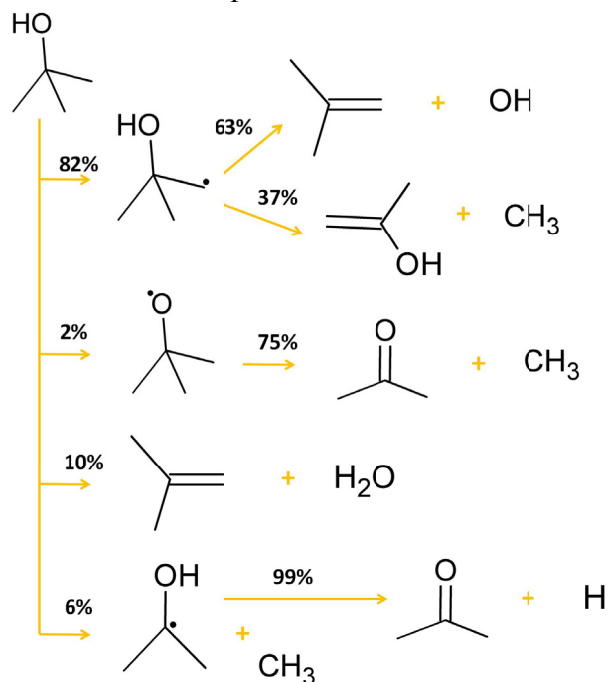


Figure 12. Fuel cracking path of *t*-butanol in the stoichiometric 1-D planar flame by with air at 1 atm and initial temperature of 353 K.

From Figure 9 it is seen that under the dominant role of β -scission, *n*-butanol cracks into C₂-C₃ species, such as ethylene (C₂H₄), propene (C₃H₆), ethanol (C₂H₃OH) and *n*-propenol (C₃H₅OH). The cracking path of *s*-butanol, shown in Figure 10, also follows almost exclusively the β -scission rule. There are four hydroxybutyl radicals for *s*-butanol: sC₄H₈OH-m, sC₄H₈OH-3, sC₄H₈OH-2 and sC₄H₈OH-1. The first three crack into C₂ species, 1-butene and 2-butene; however, sC₄H₈OH-1 cracks into *iso*-propenol (iC₃H₅OH), which is then partially converted into acetone (CH₃COCH₃). There are three hydroxybutyl radicals for *i*-butanol: iC₄H₈OH-1, iC₄H₈OH-2 and iC₄H₈OH-3. It is seen from Figure 11 that while iC₄H₈OH-3 cracks into straight chain species, iC₄H₈OH-1, iC₄H₈OH-2 can lead to large amount of *iso*-butene (iC₄H₈) and similar branched C₄ alcohols. Since *t*-butanol is a highly branched fuel, all of its initial crack paths result in branched species: *iso*-butene (iC₄H₈), *iso*-propenol (iC₃H₅OH) and acetone (CH₃COCH₃), as shown in Figure 12. The main path for *t*-butanol is through tC₄H₈OH, which cracks into *iso*-butene (iC₄H₈) and *iso*-propenol (iC₃H₅OH). Figure 12 in addition shows that 10% of *t*-butanol also dissociates into *iso*-butene (iC₄H₈) and H₂O, through the water elimination reaction because the C-O bond in *t*-butanol is relatively weak [23].

The above analysis then satisfactorily explains the role of the molecular structure of the butanol isomers on the ordering of their laminar flame speeds. Since the C-O bond is stronger than the C-C bond but weaker than the C-H bond, the role of O in the isomers is similar to that of C in the initial fuel cracking process. In this sense, if we consider the chain structure formed by the C-C and C-O bonds, only *n*-butanol has the straight chain structure, whereas *s*-butanol, *i*-butanol and *t*-butanol all crack into various amount of branched intermediate species, which are kinetically more stable.

5. Conclusions

Using expanding spherical flames, laminar flame speeds and Markstein lengths for *n*-butanol, *s*-butanol, *i*-butanol and *t*-butanol were determined at pressures from 1 atm to 5 atm over a wide range of equivalence ratios. Results at all pressures show that *n*-butanol has the highest flame speed, followed by *s*-butanol and *i*-butanol, and then *t*-butanol; with the flame speeds of *s*-butanol and *i*-butanol being almost the same. Calculated values yield satisfactory agreement with the present data for all fuels at all pressures, especially their ordering, with a slight over-prediction for *n*-butanol and *s*-butanol. The ordering also agrees with measurements of Veloo *et al.*[3] at 1 atm, although their values are slightly higher than the present data for *n*-butanol, *s*-butanol and *i*-butanol. This ordering, however, does not agree with measurements of Gu *et al.*[6].

Results also show that the Markstein lengths of *n*-butanol are considerably lower for the data obtained at 5 atm with oxygen-helium-argon mixture as the oxidizer. However, this lower Markstein length is caused by the reduced flame thickness for *n*-butanol such that the Markstein numbers (Markstein lengths scaled by flame thickness) of *n*-butanol are similar to those of other fuels. This

indicates that the butanol isomers have similar nonequidiffusive properties when subjected to aerodynamic stretching.

Calculation also shows that the difference in adiabatic flame temperatures accounts for approximately 20% of the difference in the laminar flame speeds among the isomers, implying that kinetics is the main reason for the difference in the flame speeds. Sensitivity coefficients for reaction rates on flame speeds, intermediate species distributions and reaction paths were evaluated for all the isomers. It is concluded that the difference in the flame speed is due to the fact that *n*-butanol is the only straight chain fuel which readily cracks into reactive straight chain species, while *s*-butanol, *i*-butanol and *t*-butanol are all branched molecules and crack into relatively more stable branched intermediate species, such as *iso*-butene, *iso*-propenol and acetone. The resulting flame speed then depends on the extent of the fuel molecule branching, with *t*-butanol having the most branched structure and thus the lowest flame speed.

Acknowledgements

This work was supported by the Combustion Energy Frontier Research Center, an Energy Frontier Research Center funded by the US Department of Energy, Office of Basic Energy Sciences under Award Number DESC0001198. The authors would like to thank Professor Mani Sarathy for providing help in using the butanol mechanism, to Professor Yiguang Ju for the use of the PLOG Chemkin code, and to Roe Burrell for helping solving problems in running it.

References

- [1] P.S. Nigam, A. Singh, Progress in Energy and Combustion Science. 37 (2011) 52-68.
- [2] S.M. Sarathy, M.J. Thomson, C. Togbé, P. Dagaut, F. Halter, C. Mounaim-Rousselle, Combustion and Flame. 156 (2009) 852-864.
- [3] P.S. Veloo, F.N. Egolfopoulos, Proceedings of the Combustion Institute. 33 (2011) 987-993.
- [4] W. Liu, A.P. Kelley, C.K. Law, Proceedings of the Combustion Institute. 33 (2011) 995-1002.
- [5] X. Gu, Z. Huang, Q. Li, C. Tang, Energy & Fuels. 23 (2009) 4900-4907.
- [6] X. Gu, Z. Huang, S. Wu, Q. Li, Combustion and Flame. 157 (2010) 2318-2325.
- [7] X. Gu, Q. Li, Z. Huang, Combustion Science and Technology. 183 (2011) 1360-1375.
- [8] X. Gu, Q. Li, Z. Huang, N. Zhang, Energy Conversion and Management. 52 (2011) 3137-3146.
- [9] A.P. Kelley, A.J. Smallbone, D.L. Zhu, C.K. Law, Proceedings of the Combustion Institute. 33 (2011) 963-970.
- [10] F. Wu, A.P. Kelley, C.K. Law, Combustion and Flame. 159 (2012) 1417-1425.
- [11] A.P. Kelley, J.K. Bechtold, C.K. Law, 7th U.S. National Combustion Meeting, 2011.
- [12] A.P. Kelley, G. Jomaas, C.K. Law, Combustion and Flame. 156 (2009) 1006-1013.
- [13] M.P. Burke, Z. Chen, Y. Ju, F.L. Dryer, Combustion and Flame. 156 (2009) 771-779.
- [14] Z. Chen, M.P. Burke, Y. Ju, Proceedings of the Combustion Institute. 32 (2009) 1253-1260.
- [15] A.P. Kelley, Dynamics of Expanding Flames, Ph.D. Dissertation, Princeton University, 2011.
- [16] R.J. Kee, J.F. Grcar, M.D. Smooke, J.A. Miller, E. Meeks. Sandia report 85-8240., 1985.
- [17] S.M. Sarathy, S. Vranckx, K. Yasunaga, M. Mehl, P. Oßwald, W.K. Metcalfe, et al., Combustion and Flame. 159 (2012) 2028-2055.
- [18] X. Gou, J.A. Miller, W. Sun and Y. Ju, <http://engine.princeton.edu>, 2011.

- [19] M. Matalon, C. Cui, J.K. Bechtold, *Journal of Fluid Mechanics*. 487 (2003) 179-210.
- [20] C. Ji, S.M. Sarathy, P.S. Veloo, C.K. Westbrook, F.N. Egolfopoulos, *Combustion and Flame*. 159 (2012) 1426-1436.
- [21] S.G. Davis, C.K. Law, *Combustion Science and Technology*. 140 (1998) 427-449.
- [22] J.K. Lefkowitz, J.S. Heyne, S.H. Won, S. Dooley, H.H. Kim, F.M. Haas, et al., *Combustion and Flame*. 159 (2012) 968-978.
- [23] I. Glassman, R.A. Yetter, *Combustion*, Academic Press, New York, 2008.